FRONT TRACKING AND OPERATOR SPLITTING FOR NONLINEAR DEGENERATE CONVECTION–DIFFUSION EQUATIONS

S. EVJE, K. HVISTENDAHL KARLSEN, K.–A. LIE, AND N. H. RISEBRO

ABSTRACT. We describe two variants of an operator splitting strategy for nonlinear, possibly strongly degenerate convection–diffusion equations. The strategy is based on splitting the equations into a hyperbolic conservation law for convection and a possibly degenerate parabolic equation for diffusion. The conservation law is solved by a front tracking method, while the diffusion equation is here solved by a finite difference scheme. The numerical methods are unconditionally stable in the sense that the (splitting) time step is not restricted by the spatial discretization parameter. The strategy is designed to handle all combinations of convection and diffusion (including the purely hyperbolic case). Two numerical examples are presented to highlight the features of the methods, and the potential for parallel implementation is discussed.

1. INTRODUCTION

We consider nonlinear convection–diffusion equations of the type

$$\partial_t u + \sum_{i=1}^{d} \partial_{x_i} F_i(x,u) = \varepsilon \sum_{i=1}^{d} \partial_{x_i}^2 A_i(x,u), \quad x \in \mathbb{R}^d, t \in \langle 0, T \rangle, \tag{1}$$

with initial data $u(x,0) = u_0(x)$. Here $u_0(x)$ is a bounded function of bounded total variation, F_i and A_i are sufficiently regular and $\partial_u A_i$ is non-negative for all i. The small scaling parameter $\varepsilon > 0$ indicates convection dominated flow.

When (1) is non-degenerate, that is, $\partial_u A_i \geq \eta > 0$ for all i, it is well known that the equation admits classical solutions. This contrasts with the case where (1) is allowed to degenerate for some values of u. The simplest examples are perhaps provided by the porous medium equation $u_t = \varepsilon(u^m)_{xx}$, and the convective porous medium equation $u_t + (u^n)_x = \varepsilon(u^m)_{xx}$, which both degenerate at $u = 0$ for $n, m > 1$. In general, a manifestation of degeneracy is the finite speed of propagation of disturbances. Thus, if at some fixed time the solution u has compact support, then it will continue to have compact support for all later times. The transition from a region where $u > 0$ to one where $u = 0$ is not smooth and it is therefore necessary to deal with weak solutions rather than classical solutions. We refer to the review papers [16, 21] and references cited therein for an overview of the mathematical theory of degenerate equations.

If (1) is strongly degenerate, that is, $\partial_u A_i = 0$ for all u in an interval $[\alpha, \beta]$ for some i, solutions can develop singularities in finite time. A striking feature of such equations is that weak solutions are not necessarily unique. Accordingly, one must require some admissibility criteria to single out the physically relevant weak solution. The viscosity criterion seeks weak

Key words and phrases. Degenerate convection–diffusion equations, operator splitting, front tracking, finite difference method, oil reservoir simulation.

solutions to (1) as the L_1 limits of smooth solutions u^μ to non-degenerate parabolic equations,

$$\partial_t u^\mu + \sum_{i=1}^d \partial_{x_i} F_i(x,u^\mu) = \varepsilon \sum_{i=1}^d \partial_{x_i}^2 A_i(x,u^\mu) + \mu \sum_{i=1}^d \partial_{x_i}^2 u^\mu,$$

as the parabolic regularization parameter $\mu > 0$ tends to zero. It turns out that this viscosity approach yields the following entropy admissibility criterion: We call a bounded measurable function $u(x,t)$ an *entropy weak solution* of (1) if the (entropy) inequality

$$\begin{aligned}\partial_t |u-k| + \sum_{i=1}^d \partial_{x_i} \left[\operatorname{sgn}(u-k)(F_i(x,u) - F_i(x,k)) \right] \\ -\varepsilon \sum_{i=1}^d \partial_{x_i}^2 |A_i(x,u) - A_i(x,k)| \\ + \sum_{i=1}^d \operatorname{sgn}(u-k)(F_{ix_i}(x,k) - \varepsilon A_{ix_ix_i}(x,k)) \le 0\end{aligned}$$

holds in the distributional sense for all $k \in \mathbb{R}$. The notion of an entropy weak solution includes all the previously mentioned parabolic equations as well as hyperbolic conservation laws in the sense of Kruzkov [28]. It thus provides a suitable framework for analysing numerical methods that are especially designed to handle mixed type convection–diffusion equations. We refer to Refs. [34, 35, 37] for theory of strongly degenerate equations.

We shall here restrict ourselves to a physically reasonable class of equations in which the functions F_i and A_i have the form $F_i(x,u) = V_i(x) f_i(u)$ and $A_i(x,u) = A_i(u) = \int_0^u a_i(\xi)\, d\xi$ for some bounded functions V_i and a_i. Equation (1) can then be rewritten as

$$\partial_t u + \sum_{i=1}^d V_i(x) \partial_{x_i} f_i(u) = \varepsilon \sum_{i=1}^d \partial_{x_i} (a_i(u) \partial_{x_i} u) + G(x,u), \tag{2}$$

where $G = -\sum_i V_i(x)_{x_i} f_i(u)$. Our numerical strategy is essentially based on splitting (2) into a hyperbolic conservation law for convection and a parabolic equation for diffusion (and source). We then try to reproduce the solution using numerical methods for these simpler equations as building blocks. Variations on this operator splitting approach have indeed been taken in various contexts, for instance for Navier–Stokes flow [2, 3, 38] and for flow in porous media [5, 7, 8, 15, 33]. An approach similar to the one we advocate here is that of Dawson et al. [6, 36], who employ a Godunov method for the convection step.

The purpose of our paper is to continue—and improve—the work initiated recently by Karlsen et al. [23, 24, 25, 26], which is based on a front tracking method for the convection step and a finite element or a difference method for the diffusion step. For an overview of the this activity we refer to the lecture notes by Espedal and Karlsen [9]. All previous works have mainly focused on non-degenerate equations or special equations possessing a one or two point degeneracy. Recently, we started investigating the convergence properties of splitting methods for strongly degenerate convection–diffusion equations [14, 18]. In particular, a fully discrete splitting method for (1) was proposed and analysed in [18]. In the current paper we *demonstrate* two versions of this splitting method that differ only in the way the dimensional splitting part is carried out. For the diffusive part we rely on an explicit finite difference

scheme coupled with a super time stepping acceleration procedure [1]. Finite difference approximations of entropy solutions of strongly degenerate convection-diffusion equations have been analysed by Evje and Karlsen in a series of papers [13, 10, 12, 11].

Two numerical examples are presented and discussed. In the first example, the methods are used to compute discontinuous entropy solutions of a two-dimensional Burgers type equation with a strongly degenerate second order term. The second example is a parabolic–elliptic system of equations describing two-phase flow of water and oil in an oil reservoir. More numerical experiments are given in [19].

A reason for using front tracking is that this method has no time step restriction. Accordingly, our splitting methods are unconditionally stable in the sense that the splitting time step is not limited by the spatial discretization parameter. Tests with CFL numbers varying in the range $\frac{1}{2}$ to 32 show that large CFL numbers are indeed feasible for the problem in Example 1.

For non-degenerate parabolic equations, viscous splitting errors introduced by using large time steps may lead to shock fronts that are too wide. For one of the methods, this potential problem is easy to overcome. In the second example we demonstrate a 'correction' technique that substantially decreases the viscous error contribution and thus makes large splitting steps feasible.

We then address the issue of parallel implementation of the methods. Idealised, both splitting methods are 'perfect' for parallel implementation. However, given a certain architecture, there are important practical issues that have to be resolved.

Our paper is organized as follows. In §2 we describe in detail our numerical methods. In §3 we present and discuss the numerical examples. Finally, in §4 we discuss parallel aspects of our methods.

2. The Numerical Algorithms

Our splitting techniques result in two different equations that each must be solved numerically. Therefore, before we describe the splitting algorithms in more detail, we introduce numerical schemes for these two equations.

2.1. **The Hyperbolic Solver.**

Let us begin with front tracking for the convection part. Consider therefore the one-dimensional conservation law

$$\partial_t v + V(x)\partial_x f(v) = 0, \quad v(x,0) = v_0(x), \quad x \in \mathbb{R},\ t > 0. \tag{3}$$

In the front tracking approach, we seek approximations to (3) within the class of step functions. To this end, we approximate the initial data by a step function v_0^h to decompose the initial value problem into a sequence of simple Riemann problems. By approximating the flux function by a piecewise linear function f^δ, we ensure that the solution of each Riemann problem is a step function. The global solution—until the first wave interaction occurs—thus consists of constant states separated by discontinuities propagating along paths $x(t)$. Each path $x(t)$ is given by the differential equation $\dot{x} = V(x)s$, where s is the Rankine–Hugoniot speed $(f^\delta(u_L) - f^\delta(u_R))/(u_L - u_R)$. If the velocity V is approximated by either a piecewise constant or a piecewise linear function V^δ, the differential equations can be solved explicitly and the paths $x(t)$ are given in closed form.

So far, we have constructed a solution that is valid until the first wave interaction occurs, but since the wave interaction merely defines a new Riemann problem, this and all future interactions can be resolved as above. In fact, it can be shown [17, 29] that there is a finite

number of wave interactions, even in infinite time, if the initial data is bounded and has finite total variation. Hence, tracking discontinuities and solving Riemann problems will take us up to any desired time t. In this approach, rarefaction waves are approximated by sequences of small shocks. Moreover, there is no time step associated with the method. Front tracking for $V \equiv 1$ is described and analysed in detail by Holden et al. [17] and an error estimate is provided by Lucier [32]. Lie [29] extended the method to $V = V(x,t)$.

To solve multi-dimensional conservation laws of the form

$$\partial_t v + \sum_{i=1}^{d} V_i(x)\partial_{x_i} f_i(v) = 0, \quad v(x,0) = v_0(x), \quad x \in \mathbb{R}^d,\ t > 0,$$

we use the above method combined with dimensional splitting. Introduce a uniform Cartesian grid with discretization parameter $h > 0$ in each direction and a time step $\Delta t > 0$. Let π be the usual grid cell averaging operator. The multi-dimensional front tracking solution, which is a piecewise constant function on the Cartesian grid, is then given by the following dimensional splitting formula

$$v(x, n\Delta t) \approx \left[\pi \circ \mathcal{S}_{\Delta t}^{x_d,h} \cdots \pi \circ \mathcal{S}_{\Delta t}^{x_1,h}\right]^n \pi v_0,$$

where $\mathcal{S}_t^{x_i,h}$ denotes the front tracking operator at time t applied in the ith direction.

Although a time step is associated with the multi-dimensional method, it is unconditionally stable in the sense that the time step is not restricted by a CFL condition. This contrasts strongly with typical difference methods for conservation laws. Previous studies have shown that shock waves can advantageously be propagated using CFL numbers as high as 10–20 (see [31]). The multi-dimensional front tracking method is described and analysed by Holden and Risebro [20] for $V = 1$ and by Lie [30] for general $\nabla \cdot V = 0$. An error estimate is derived in Refs. [22, 31].

2.2. **The Parabolic Solver.** The diffusion step is realized by solving a nonlinear, possibly strongly degenerate, parabolic equation of the form

$$\begin{aligned} \partial_t w &= \varepsilon \sum_{i=1}^{d} \partial_{x_i}(a_i(w)\partial_{x_i} w) + G(x,w), \\ w(x,0) &= w_0(x), \quad x \in \mathbb{R},\ t > 0. \end{aligned} \tag{4}$$

The difference method uses a uniform Cartesian grid with grid cell size $h > 0$ in each direction, and a time step $k > 0$. Let W^n denote the finite difference solution at time $t = nk$. Let $\Delta_{-,i}$ and $\Delta_{+,i}$ be the usual ith directional backward and forward difference operators, respectively. Then we define W^{n+1} by the following difference formula

$$W^{n+1} = \varepsilon \frac{k}{h^2} \sum_{i=1}^{d} \Delta_{-,i}\Delta_{+,i} A_i^n + kG^n,$$

where A_i^n and G^n have obvious meanings. To ensure stability we must choose h and k so that $2d\varepsilon(k/h^2)\max_{i,u}|a_i(u)| \le 1$, see, e.g., [13]. The method is initiated by letting $W^0 = \pi w_0$. Note that we insist on working with the conservation form of (4) when defining the difference method.

Super Time Stepping Acceleration. Super time stepping (STS) is an efficient way to speed up explicit schemes for parabolic problems. The STS procedure relaxes the restrictive stability condition associated with the explicit scheme so that the resulting diffusion solver runs at least as fast and is of comparable or better accuracy than the corresponding implicit diffusion solver.

The idea is quite simple, for more details see Alexiades et al. [1]. Let us consider the time dependent problem $\dot{U} + AU(t) = 0$, $U(0) = U_0$ discretized by the forward Euler method

$$U^{n+1} = U^n - \tau A U^n, \qquad U^0 = U_0.$$

This method is stable if the spectral radius $\rho(I - \tau A)$ is less than unity, which is fulfilled if $\tau < \tau_e = 2/\lambda_{\max}$, where $\lambda_{\max}$ is the largest eigenvalue of A.

We now introduce a cycle of N intermediate time steps $\{\tau_i\}_{i=1}^N$ and a corresponding *super-step* $\Delta T = \sum_{i=1}^N \tau_i$. The stability requirement is then imposed on ΔT rather than on τ. The new scheme becomes

$$U^{n+1} = \Big(\prod_{i=0}^{N}(I - \tau_i A)\Big)U^n, \qquad U^0 = U_0.$$

The corresponding stability condition is $\rho(\prod_{i=0}^N (I - \tau_i A)) < 1$. We then try to maximize the length of the superstep ΔT such that $\Delta T \geq N\tau_e$. It turns out that this is achieved if the τ_i's are given by the formula

$$\tau_i = 2\Big((-1+\nu)\cos\big(\frac{2i-1}{N}\frac{\pi}{2}\big) + 1 + \nu\Big)^{-1}, \qquad i = 1, \ldots, N.$$

The parameters N and ν determine speedup in the acceleration. Note that $N = 1$ and $\nu = 0$ corresponds to the standard explicit scheme. Since ΔT tends to $N^2\tau_e$ as $\nu \to 0$, super stepping is up to N times faster than the standard explicit scheme. Moreover, the method is fairly robust with respect to the parameters, and no precise knowledge regarding the properties of A is needed when choosing N and ν. Although the method can only be justified theoretically for linear problems, it appears to be applicable to nonlinear problems as well, see Ref. [1]. This is also confirmed by numerical experiments in §3.

2.3. **The Splitting Techniques.** From now on let $h > 0$ and $\Delta t > 0$ denote the spatial and temporal discretization parameters associated with our discrete splitting methods. As above, let $\mathcal{S}_t^{x_i,h}$ denote the front tracking solution operator associated with the one-dimensional hyperbolic conservation law at time t

$$\partial_t v + V_i(x)\partial_{x_i} f_i(v) = 0, \quad x_i \in \mathbb{R},\ t > 0.$$

Similarly, let $\mathcal{H}_t^{x_i,h}$ denote the finite difference solution operator of

$$\partial_t w = \varepsilon \partial_{x_i}(a_i(w)\partial_{x_i} w), \quad x_i \in \mathbb{R},\ t > 0$$

and $\mathcal{H}_t^{x,h}$ the finite difference solution operator of

$$\partial_t w = \varepsilon \sum_{i=1}^{d} \partial_{x_i}(a_i(w)\partial_{x_i} u) + G(x, w), \quad x \in \mathbb{R}^d,\ t > 0.$$

Moreover, let $\mathcal{R}_t^h$ denote the solution operator of

$$r_t = G(x, r), \quad x \in \mathbb{R}^d,\ t > 0.$$

We then introduce the following two operator splitting methods

$$u(x, n\Delta t) \approx \left[\mathcal{H}^{x,h}_{\Delta t} \circ \pi \circ \mathcal{S}^{x_d,h}_{\Delta t} \cdots \pi \circ \mathcal{S}^{x_1,h}_{\Delta t}\right]^n \pi u_0 \equiv u^n \tag{5}$$

and

$$u(x, n\Delta t) \approx \left[\mathcal{R}^{h}_{\Delta t} \circ \mathcal{H}^{x_d,h}_{\Delta t} \circ \pi \circ \mathcal{S}^{x_d,h}_{\Delta t} \cdots \mathcal{H}^{x_1,h}_{\Delta t} \circ \pi \circ \mathcal{S}^{x_1,h}_{\Delta t}\right]^n \pi u_0 \equiv u^n. \tag{6}$$

Henceforth the methods will be referred to as the unsplit (5) and the split (6) method respectively, due to their different treatment of the diffusive forces. Various convergence results for these splitting methods in the framework of classical solutions can be found in Refs. [23, 25, 26]. In the framework of entropy weak solutions, similar results can be found in Evje and Karlsen [14] and Holden et al. [18].

Let the sequence $\{u_\Delta(x,t)\}$, $\Delta = (h, \Delta t)$, be defined by

$$u_\Delta(x,t) = u^n(x), \quad \text{for } (x,t) \in \mathbb{R}^d \times ((n-1)\Delta t, n\Delta t), \qquad n = 1, \ldots, N,$$

where u^n is given by (5) or (6) and $n\Delta t = T$. Then there exists a subsequence $\{u_{\Delta_j}(x,t)\}$ converging almost everywhere on $\mathbb{R}^d \times \langle 0, T\rangle$ to a bounded measurable function $u(x,t)$. Moreover, the limit function $u(x,t)$ is an entropy weak solution of the convection–diffusion problem (1). See [18] for more details.

3. Applications

We now present and discuss two numerical examples. The first example clearly demonstrates that our methods can handle equations with strongly degenerate diffusion terms. The qualitative behaviour of solutions to degenerate parabolic equations is poorly understood, as opposed to hyperbolic conservation laws and non-degenerate parabolic equations. We here use our solution technique to construct a *discontinuous* entropy solution.

The second example is a parabolic–elliptic system of partial differential equations, which is used in the simulation of certain secondary oil recovery processes. The purpose is to demonstrate an application of our strategy to a realistic problem. Moreover, the example presents techniques for reducing viscous splitting errors, which unattended might have been a significant drawback of our numerical strategy.

The simulations below use relatively fine grids, which is *not* a prerequisite for our methods. In the first example we simply seek high resolution when describing solutions qualitatively. In the second example we seek to eliminate most of the spatial error contribution and thus enhance the temporal splitting error, which is our main concern here.

Example 1: Strongly degenerate diffusion. Consider the two-dimensional Burgers type problem

$$\partial_t u + \partial_x(u^2) + \partial_y(u^2) = \varepsilon \partial_x(a(u)\partial_x u) + \varepsilon \partial_y(a(u)\partial_y u),$$

where $\varepsilon = 0.1$ and the diffusion coefficient is strongly degenerate

$$a(u) = \begin{cases} 0, & \text{for } |u| \le 0.25, \\ 1, & \text{for } |u| > 0.25. \end{cases}$$

The equation is therefore of hyperbolic nature when $u \in [-0.25, 0.25]$ and parabolic elsewhere. The initial data is equal -1 and 1 inside two circles of radius 0.4 centred at $(0.5, 0.5)$ and $(-0.5, -0.5)$, respectively, and zero elsewhere inside the square $[-1.5, 1.5] \times [-1.5, 1.5]$.

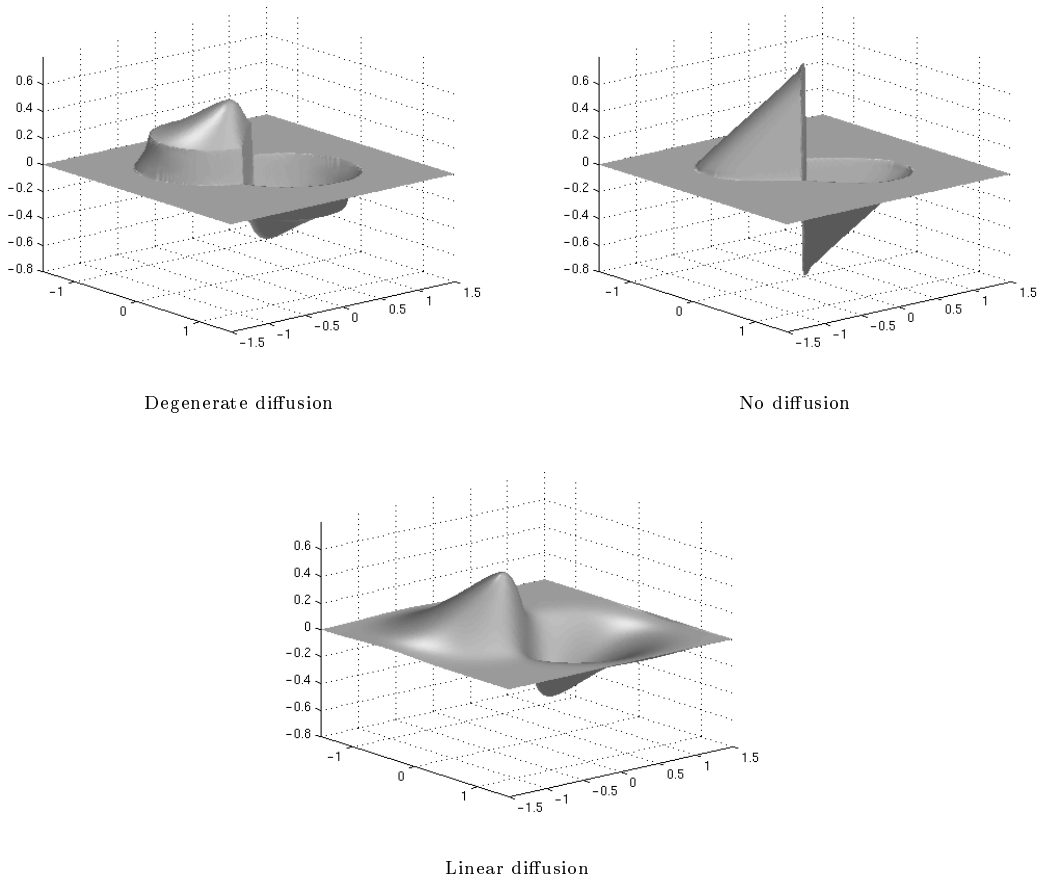

FIGURE 1. Solution at times t=0.5 on a 200*200 grid.

The qualitative nature of the degenerate problem differs from the pure hyperbolic problem ($a(u) \equiv 0$) and the non-degenerate parabolic problem ($a(u) \equiv 1$). Figure 1 shows a surface plot of the three solutions at time $t = 0.5$ on a fine grid and Figure 2 shows the development along the diagonal line $x = y$. The nonlinear flux function will cause the two cylinders to deform and move towards the origin. Due to the degenerate diffusion coefficient, the leading front of each cylinder is discontinuous and propagates at a finite velocity (as opposed to the linear diffusion case). As the two leading fronts reach the line $x = -y$, they interact and produce a stationary shock, as in the hyperbolic case. The trailing edges are rarefaction waves in the intervals $[0, 0.25]$ and $[-0.25, 0]$, respectively, but the waves move slower than in the hyperbolic case because of the interaction with the parabolic region. Moreover, note the lack of smoothness at $u = \pm 0.25$. In the two parabolic regions $|u| > 0.25$, the solution will be dissipated and decrease in absolute value towards 0.25. After a while, the parabolic regions have disappeared and the solution consists of two rarefaction waves separated by a shock. The height of the shock decreases and asymptotically the solution tends to $u \equiv 0$.

The solution is symmetric with respect to the diagonal. Both solution strategies (5) and (6) involve dimensional splitting, and we thus expect a lack of symmetry. Here $U^n_{i,j}$ denotes the solution in grid block (i, j) at time $n\Delta t$. The quality of numerical solutions are

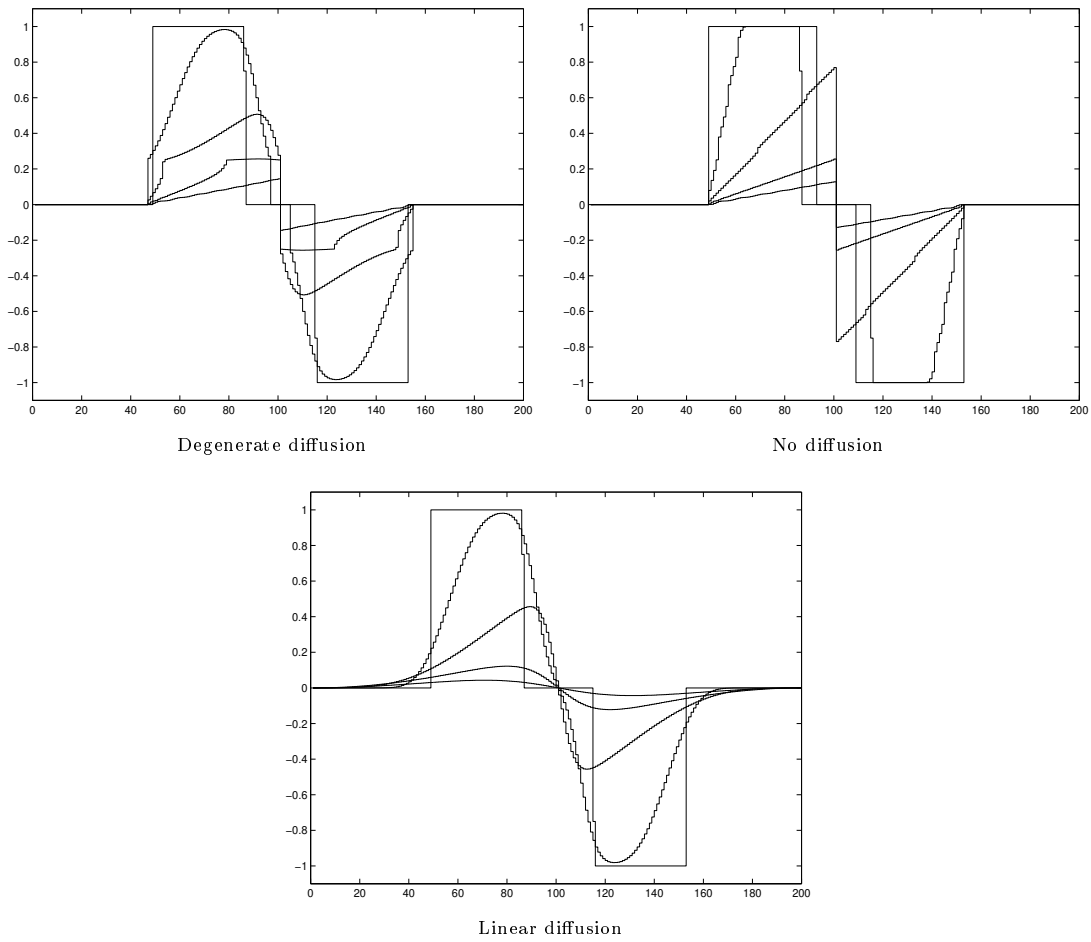

FIGURE 2. Solution at times t=0.0, 0.1, 0.5, 1.5, and 3.0 along the diagonal on a 200*200 grid.

TABLE 1. *Numerical errors for the two different splitting algorithms at times* $t = 0.5$ *(top) and* $t = 1.0$ *(bottom).* E_1 *is* L_1 *error and* E_s *is symmetry error. STS parameters are* $N = 4$ *and* $\nu = 0.002$.

		Method (5)		Method (6)	
Grid	Steps	E_1	E_s	E_1	E_s
50	5	8.0e-02	3.1e-02	9.4e-02	1.3e-01
100	10	4.7e-02	2.0e-02	4.6e-02	6.5e-02
200	20	2.1e-02	8.6e-03	2.2e-02	3.3e-02
50	10	6.8e-02	3.7e-02	9.7e-02	1.3e-01
100	20	3.2e-02	1.5e-02	4.5e-02	6.7e-02
200	40	1.2e-02	4.5e-03	2.1e-02	3.5e-02

measured in the L_1 norm. In addition we introduce the symmetry error, here defined as $E_s = \sum_{i,j} |U^n_{i,j} - U^n_{j,i}|h^2$. Table 1 gives the symmetry error and the L_1 error with respect to a

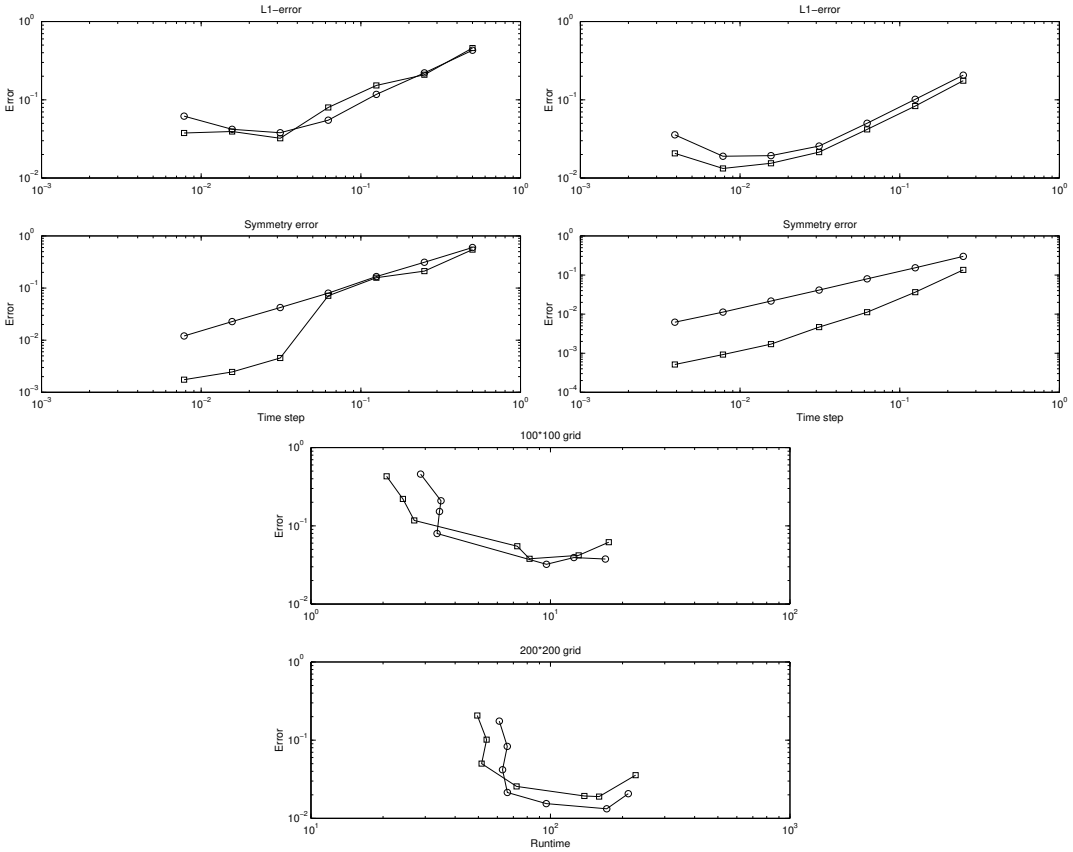

FIGURE 3. Numerical errors at time $t = 0.5$ for different time steps on fixed grids; a 100*100 grid (left), a 200*200 grid (right), and error versus runtime (bottom). Squares are for the unsplit method and circles for the split method. The time steps corresponds to CFL numbers $\frac{1}{2}, 1, 2, \ldots, 32$. The STS parameters are $N = 4$ and $\nu = 0.02$ and $N = 8$ and $\nu = 0.04$, respectively.

fine grid reference solution for runs with CFL number 3.3 on three grids for the two splitting methods.

As expected the symmetry is better preserved using (5), since the diffusion step is multi-dimensional. The L_1 errors are also better for the unsplit method. The measured convergence rates indicate convergence of order 1. However, if runtime is taken into account, the two methods have almost equal performance with respect to L_1 error for a wide range of CFL numbers (see below).

As pointed out before, the time step is not restricted by the spatial discretization parameter and is therefore a free parameter that must be chosen. There are two obvious sources of error in the calculation that effects this choice; the splitting error increases with the time step and the projection error decreases. A previous study for hyperbolic equations [31] shows that the best L_1 accuracy is achieved for splitting steps with CFL number moderately above unity and that the accuracy is not significantly reduced if the step is chosen even larger.

Figure 3 shows that a similar observation can be made here. As expected, the symmetry error increases with increasing time step. The minimum L_1 error is achieved for CFL number

1 or 2. However, plotting the L_1 error versus the runtime gives a minimum for a CFL number 10–20. There are two reasons for this. First, the wave structure is relatively simple so that only a few waves interact for *any* size of the time step. Therefore large time steps give a reduced number of operations in the hyperbolic part. Second, with large steps it is possible to gain more in efficiency by applying super-time-stepping acceleration in the diffusion solver. Both methods benefit from using the STS method—typically a speedup of factor 2–4 was observed.

Large time steps may introduce considerable viscous splitting error in the form of too wide (parabolic) shock layers. This effect is hardly evident here because the time step typically is of the same order as ε. Moreover, the shock fronts are mainly located in the hyperbolic region where there is no viscous error. In the next example, we demonstrate a technique for the split method that greatly reduces potential viscous splitting errors.

Example 2: Secondary oil recovery. Consider two-phase immiscible, incompressible flow of oil and water in a two-dimensional oil reservoir, or more specific, consider a variant of the widely used quarter five–spot test case. Water injection can be described by a coupled system of nonlinear partial differential equations [4]. The elliptic pressure equation

$$\nabla\big((\lambda_w + \lambda_o)\nabla p\big) = 0$$

is coupled to the parabolic saturation equation

$$\partial_t s + \nabla(V f(s)) = \varepsilon \nabla \cdot (D \nabla s)$$

via the total Darcy velocity $V = -(\lambda_w + \lambda_o)\nabla p$, and the unknowns are the global pressure p and the water saturation s. The mobilities of water λ_w and oil λ_o are fluid properties that are known functions of s. The fractional flow function $f(s) = \lambda_w/(\lambda_w + \lambda_o)$ and the diffusion tensor $D(x, s)$ are also known functions of s. The small scaling parameter $\varepsilon > 0$ gives the relative balance between convective and (diffusive) capillary forces. As a simple model, we will use $D \equiv 1$, $\varepsilon = 0.01$, $\lambda_w(s) = s^2$, and $\lambda_o(s) = (1-s)^2$. In particular, this means that the shock fronts will be purely parabolic.

The two equations are decoupled by a sequential time stepping procedure—the so-called IMPES method [4]. The initial saturation is used as input in the pressure equation to solve for the Darcy velocity. Then the saturation equation is solved with V held constant. The pressure is then recomputed using the saturation as input, and so on. Ref. [27] gives a rigorous treatment of this procedure (in the non-degenerate case). We are merely interested in the saturation equation and assume that the velocity is a given quantity that fulfils a 'no flow' condition ($V \cdot n = 0$) on the boundary. Below, the velocity has been generated by a Galerkin finite element solver.

The quarter five–spot test case is a unit reservoir with an injection well placed at $(0, 0)$ and a production well at $(1, 1)$. Both wells have unit rates and are modelled as inflow/outflow boundaries. Away from the wells we require a 'no flow' condition. The saturation is zero initially inside the reservoir. Near the wells, the velocity approximation is poor. We therefore execute a number of small steps up to time $t = 0.01$ to establish a proper profile from the initial data. Dimensionless time 1.0 corresponds to 1.0 pore volumes injected (PVI).

Figure 4 shows contour plots of a fine grid solution at time $t = 0.1$, $t = 0.3$, and $t = 0.6$. Large velocities near the wells makes the problem highly convection dominated in the upper left and lower right corner. In the other corners, the velocities are small and the problem is diffusion dominated. Thus, the relative importance of convection versus diffusion changes

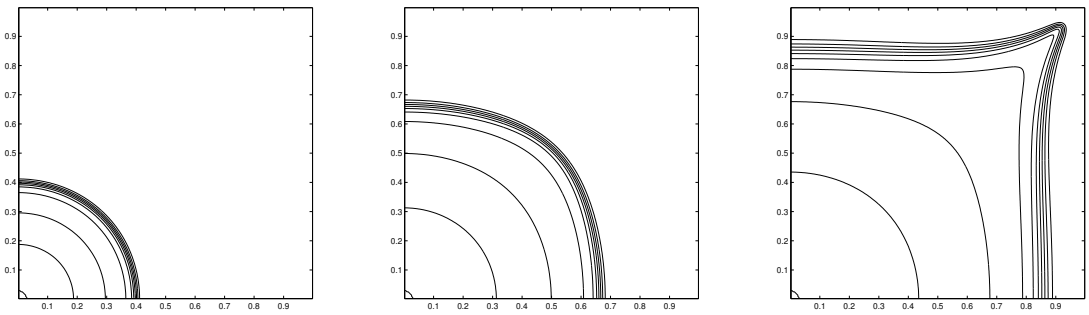

FIGURE 4. Reference solution computed by the unsplit method (5) on a 256*256 grid using 120 time steps to reach time $t = 0.6$. Snapshots at time $t = 0.1$ (left), $t = 0.3$ (middle), and $t = 0.6$ (right) with eleven evenly spaced contours.

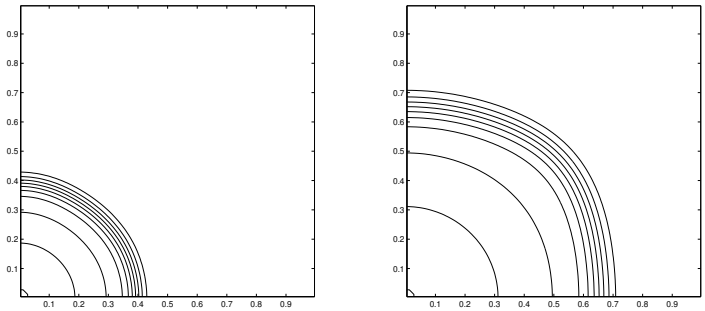

FIGURE 5. Solution computed by the unsplit method on a 128*128 grid; at time $t = 0.1$ (left) using 2 steps and at time $t = 0.3$ (right) using 2 steps in the time interval $[0.1, 0.3]$.

during the simulation. However, since the time step is less than ε, the scheme resolves the different balances accurately in all regions.

Next we investigate what happens if we increase the time step in the convection dominated regions. Figure 5 shows the solution computed by the unsplit method at times $t = 0.1$ and $t = 0.3$, computed with 2 and 4 steps, respectively. The solution is obviously far too diffusive. Note that this is a temporal and not a spatial error. The total mass balance errors, defined as (PVI—mass of water)/PVI, are 3.0% and 1.7% and the corresponding symmetry errors are 1.3e-03 and 4.4e-03.

The Diffusion Step Revisited. Although the operator splitting algorithms converge as various discretization parameters tend to zero (see Theorem 2.1), Figure 5 shows that they produce too diffusive solutions when the time step is large (compared to ε). This type of viscous splitting error can be traced back to the entropy condition used by the hyperbolic solver. Motivated by Espedal and Ewing [8] and Dahle [5], Karlsen and Risebro [25] suggested the so-called corrected operator splitting algorithm, in which a residual flux function is associated with each discontinuity in the solution of the hyperbolic step. These residual fluxes are subsequently taken into account in the diffusion step—or in a separate correction step [25]—to give the correct balance between diffusion and self-sharpening.

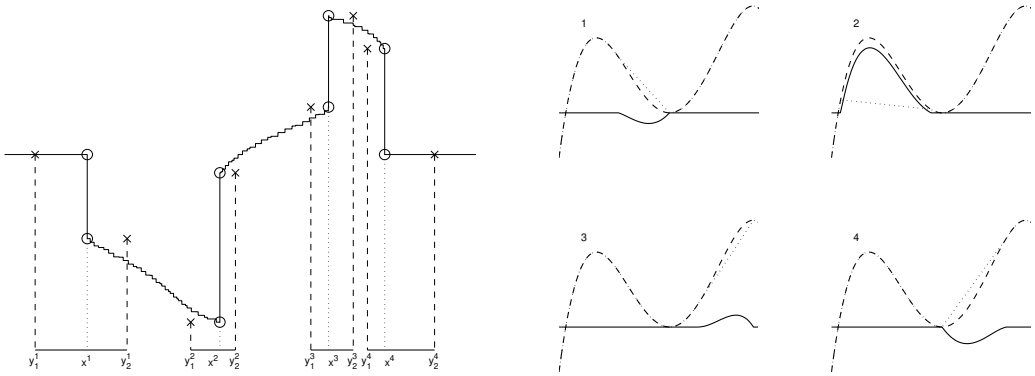

FIGURE 6. (Left) Solution from a convection step where four shocks are identified in the spatial domain. (Right) The corresponding residual flux functions: flux function (dash dotted), envelope (dotted) and residual flux function (solid).

The idea is quite simple, here explained in one dimension. Consider the solution of $v_t + f(v)_x = 0$ obtained by front tracking. Each discontinuity in v comes from a Riemann problem (v_L, v_R) that has a similarity solution $w = w(x/t)$ given by $x/t = f_c'(w(x/t))$, where f_c is the envelope function with respect to the interval $I(v_L, v_R)$. This means that because of the entropy condition, the hyperbolic solution is the same for any f that lies either below or above f_c (depending upon the data) in the interval $I(v_L, v_R)$. However, for problems with non-degenerate diffusion, the difference $f - f_c$ should not be neglected since it determines the amount of self-sharpening of fronts. Thus, one can hope to obtain the correct amount of self-sharpening by including the disregarded residual flux.

Residual flux terms can be constructed as follows. Let $v(x,t)$ be the front tracking approximation to $v_t + V(x)f(v)_x = 0$. The function $v(x,t)$ is piecewise constant on a finite number of intervals with entropy satisfying discontinuities located at $\{x^k\}$. Let v^{k+1} denote the value in $[x^k, x^{k+1}\rangle$, and let $\{(y_1^k, y_2^k)\}$ be a sequence of pairs of spatial positions chosen so that $x^k \in \langle y_1^k, y_2^k\rangle$ and $y_2^k \le y_1^{k+1}$ for all k. Then define the residual flux by

$$f^{\mathrm{res}}(x,v) = \begin{cases} f(v) - f_c(v;k), & \text{for } x \in [y_1^k, y_2^k\rangle \text{ and } v \in [v^k, v^{k+1}], \\ 0, & \text{for } x \in [y_1^k, y_2^k\rangle \text{ and } v \notin [v^k, v^{k+1}]. \end{cases}$$

Here f_c denotes the envelope of f restricted to $[v^k, v^{k+1}]$. Notice that the envelope function f_c depends on the sign of the velocity function V and the sign of $(v^k - v^{k+1})$.

In an actual implementation, all shocks with strength below a certain threshold are disregarded, i.e., we switch off all residual fluxes for which $|v^k - v^{k+1}|$ is less than some constant. Furthermore, we enlarge the spatial support of the nonzero residual fluxes, see Figure 6. The 'new' diffusion step becomes

$$\partial_t v + V(x)\partial_x f^{\mathrm{res}}(x,v) = \varepsilon \partial_x (a(u)\partial_x u) + G(x,u). \tag{7}$$

The approximate solution is constructed using the difference formula

$$W^{n+1} = -V\frac{k}{h}\Delta_0 f^{\mathrm{res}} + \varepsilon \frac{k}{h^2}\Delta_-\Delta_+ A^n + kG^n,$$

where Δ_0 is the usual central difference operator. Due to the special form of f^{res}, we see that the 'convection term' in (7) possesses the desired self-sharpening effect. Note that if

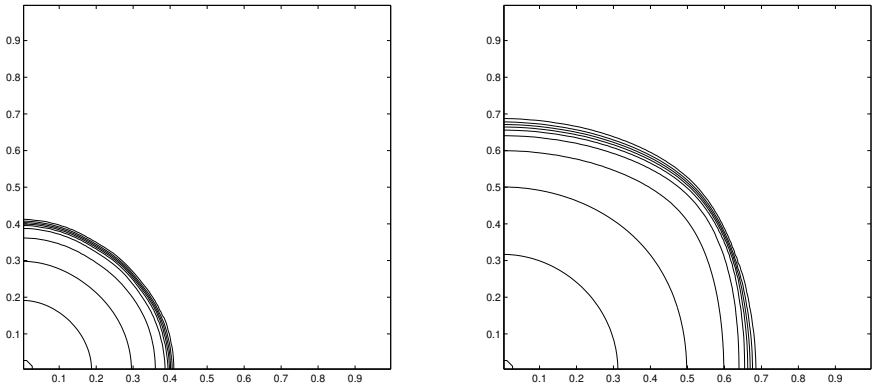

FIGURE 7. Solution at time $t = 0.1$ (left) and $t = 0.3$ (right) recomputed by COS with the same parameters as in Figure 5.

the diffusion is degenerate, one cannot use central differencing for the first order term unless an artificial diffusion term is added. An alternative approach would be to use for example Engquist–Osher differencing of the first order term, see [13, 10, 12].

The corrected splitting approach can easily be extended to arbitrary dimension using the split method (6) with the obvious modifications. Figure 7 shows the solution at times $t = 0.1$ and $t = 0.3$ recomputed using the new method with the same number of steps as above. It is evident that the correct balance between diffusion and convection is reproduced, except near the production well, where the correction is slightly too large. The improvement is remarkable compared with Figure 5 (uncorrected splitting). The mass balance errors are 2.4% and 0.87% and the symmetry errors are 7.9e-04 and 3.0e-03.

Remark 3.1. It is not obvious how to define a similar correction for the unsplit formula (5). Since the residual flux functions are generated by dimensional splitting, we cannot ensure that they are correct. Note however, that by post-processing the hyperbolic solution it is possible to devise ad hoc measures for switching off unwanted residual fluxes. Moreover, unwanted residual fluxes are not a serious problem for the current quarter five–spot case, since all waves are moving out from the injection well towards the production well. In fact, results similar to those in Figure 7 are produced, but with slightly wider shock layers. Now the mass balance errors are 2.5% and 0.92% and the symmetry errors are 2.1e-03 and 6.0e-03.

4. Parallel Aspects

Consider first the dimensional splitting method (6). Idealised, dimensional splitting has an 'infinite' potential for being parallelised. The one-dimensional problems are completely decoupled and may be solved independently. Assume that each processor may operate independent of the others (i.e., that it is of multiple instruction type) and that there are more rows/columns in the grid (from now on called tubes) than available processors. The first sweep starts by assigning a tube to each processor, which then computes the front tracking step and the finite difference step. When a processor has finished its task, it is assigned a new one. Finally, a synchronization must be issued, that is, all processors must wait for the last one to finish. Then the sweep in the next direction can be performed similarly, and so on.

There are two potential difficulties. First, the synchronization may cause problems with load balancing, unless care is taken when choosing the ratio between the number of tubes and

the number of processors. However, by assigning both the hyperbolic step *and* the diffusion step to the same processor, we ensure that the runtime is almost equal for all tubes, as the work in the front tracking step typically is just a small percentage of that of the diffusive step. Thus load balancing seems quite easy to achieve.

The second problem is the (global) communication of results after a sweep. When the sweep starts in the next direction, all processors need to know parts of the solution computed by all the others. In an idealised world, the management of data could be done by a *master* with 'unlimited' memory and communication abilities and all computations performed by *slaves* that need only know the data in one tube, or by using a shared memory approach (since no memory conflicts will arise). However, given todays technology, this will probably be a bottleneck that limits the scalability of our approach and is a very important issue when actually implementing the method on a given parallel architecture. Note, however, that the larger the time step is chosen, the fewer is the number of global communications.

The unsplit method (5) involves a different task—the multi-dimensional diffusion step. This task is quite easy, as we are using an explicit scheme; simply divide the domain into subdomains and issue each subdomain to different processors. The only communication required is that of the boundary values after each step. As long as the number of processors is not chosen too large, computation of interior points in each subdomain will dominate over the communication and the potential gain is great.

Acknowledgement

We thank Helge K. Dahle, Magne S. Espedal, Helge Holden and Johnny Frøyen for valuable discussions. We thank Jingxue Yin for interesting discussions on the theory of degenerate parabolic equations. Karlsen thanks Petter Bjørstad, Mitchell Luskin and the Institute for Mathematics and its Applications (IMA) for organising a stimulating workshop and for invitation to present some of this work. Karlsen also thanks IMA for financial support and great hospitality. This work was completed while Karlsen and Lie were guests at Institut Mittag–Leffler (ML), and they thank ML for great hospitality and NorFA for financial support.

References

[1] V. Alexiades, G. Amiez, and P. Gremaud. Super time-stepping acceleration of explicit schemes. *Com. Num. Meth. Eng.*, **12**:31–42, 1996.

[2] J.T. Beale and C. Greengard. Rates of convergence for viscous splitting of the Navier–Stokes equations. *Comm. Pure Appl. Math.*, 1083–1115, 1994.

[3] J.T. Beale and A. Majda. Rates of convergence for viscous splitting of the Navier–Stokes equations. *Math. Comp.*, **37**(156):243–259, 1981.

[4] G. Chavent and J. Jaffre. *Mathematical models and finite elements for reservoir simulation*, volume **17** of *Studies in mathematics and its applications*. North Holland, Amsterdam, 1986.

[5] H.K. Dahle. *Adaptive characteristic operator splitting techniques for convection-dominated diffusion problems in one and two space dimensions*. PhD thesis, Department of Mathematics, University of Bergen, 1988.

[6] C.N. Dawson. Godunov-mixed methods for advection–diffusion equations in multidimensions. *SIAM J. Num. Anal.*, **30**(5):1315–1332, 1993.

[7] J. Douglas and T.F. Russell. Numerical methods for convection-dominated diffusion problems based on combining the method of characteristics with finite element or finite difference procedures. *SIAM J. Num. Anal.*, **19**(5):871–885, 1982.

[8] M.S. Espedal and R.E. Ewing. Characteristic Petrov-Galerkin subdomain methods for two-phase immiscible flow. *Comput. Methods Appl. Mech. Engrg.*, **64**:113–135, 1987.

[9] M. S. Espedal and K. H. Karlsen. Numerical solution of reservoir flow models based on large time step operator splitting algorithms. In A. Fasano and H. van Duijn, editors, *Filtration in Porous Media and Industrial Applications*, Lecture Notes in Mathematics. Springer. To appear.

[10] S. Evje and K. H. Karlsen. Degenerate convection-diffusion equations and implicit monotone difference schemes. In M. Fey and R. Jeltsch, editors, *Hyperbolic problems: theory, numerics, applications (Seventh international conference in Zrich, 1998)*, ISNM Vol. 129, pp. 285–294, Birkhuser, 1999.

[11] S. Evje and K. H. Karlsen. Discrete approximations of BV solutions to doubly nonlinear degenerate parabolic equations. *Numer. Math.* Submitted.

[12] S. Evje and K. H. Karlsen. Second order difference schemes for degenerate convection-diffusion equations. Preprint 1999.

[13] S. Evje and K. H. Karlsen. Monotone difference approximations of BV solutions to degenerate convection-diffusion equations. Accepted in *SIAM J. Numer. Anal.*

[14] S. Evje and K.H. Karlsen. Viscous splitting approximation of mixed hyperbolic-parabolic convection-diffusion equations. Accepted in *Numer. Math.*

[15] R.E. Ewing. Operator splitting and Eulerian-Lagrangian localized adjoint methods for multiphase flow. In Whiteman, editor, *The Mathematics of Finite Elements and Applications VII MAFELAP*, 215–232. Academic press, San Diego, CA, 1991.

[16] B.H. Gilding. Improved theory for a nonlinear degenerate parabolic equation. *Ann. Scuola Norm. Sup. Pisa Cl. Sci.*, **16**(4):165–224, 1989.

[17] H. Holden, L. Holden, and R. Høegh-Krohn. A numerical method for first order nonlinear scalar conservation laws in one-dimension. *Comput. Math. Applic.*, **15**(6–8):595–602, 1988.

[18] H. Holden, K.H. Karlsen, and K.-A. Lie. Operator splitting methods for degenerate convection–diffusion equations I: Convergence and entropy estimates. Preprint, 1999.

[19] H. Holden, K.H. Karlsen, and K.-A. Lie. Operator splitting methods for degenerate convection–diffusion equations II: Numerical examples with emphasis on reservoir simulation. Preprint, 1999.

[20] H. Holden and N.H. Risebro. A method of fractional steps for scalar conservation laws without the CFL condition. *Math. Comp.*, **60**(201):221–232, Jan. 1993.

[21] A.S. Kalashnikov. Some results of the qualitative theory of non-linear degenerate second-order parabolic equations. *Russian Math. Surv.*, **42**:169–222, 1987.

[22] K.H. Karlsen. On the accuracy of a dimensional splitting method for scalar conservation laws. Master's thesis, Department of Mathematics, University of Oslo, 1994.

[23] K.H. Karlsen and K.-A. Lie. An unconditionally stable splitting scheme for a class of nonlinear parabolic equations. Accepted in *IMA J. Num. Anal.*

[24] K.H. Karlsen, K.-A. Lie, N.H. Risebro, and J. Frøyen. A front tracking approach to a two-phase fluid flow model with capillary forces. *In Situ*, **22**(1):59-89, 1998.

[25] K.H. Karlsen and N.H. Risebro. Corrected operator splitting for nonlinear parabolic equations. Accepted in *SIAM J. Num. Anal.*

[26] K.H. Karlsen and N.H. Risebro. An operator splitting method for convection-diffusion equations. *Numer. Math.*, **77**(3):365–382, 1997.

[27] S.N. Kružkov and S.M. Sukorjanskiĭ. Boundary value problems for systems of equations of two-phase porous flow type; statement of the problems, questions of solvability, justification of approximate methods. *Math. USSR Sbornik*, **33**(1):62–80, 1977.

[28] S.N. Kružkov. First order quasi-linear equations in several independent variables. *Math. USSR Sbornik*, **10**(2):217–243, 1970.

[29] K.-A. Lie. A front tracking method for one-dimensional nonlinear advection equations with variable coefficients. Preprint (mathematics), Norwegian University of Science and Technology, 1997.

[30] K.-A. Lie. A dimensional splitting method for quasilinear hyperbolic equations with variable coefficients. *BIT*, 39(4), 1999.

[31] K.-A. Lie, V. Haugse, and K.H. Karlsen. Dimensional splitting with front tracking and adaptive grid refinement. *Numer. Methods Partial Differential Equations*, **14**(5):627–648, 1998.

[32] B.J. Lucier. A moving mesh numerical method for hyperbolic conservation laws. *Math. Comp.*, **46**(173):59–69, Jan. 1986.

[33] T.F. Russell. Galerkin time stepping along characteristics for Burgers' equation. In Step leman et al., editor, *Scientific computing*, 183–192. IMACS, North-Holland, 1983.

[34] T. Tassa. Uniqueness of piecewise smooth weak solutions of multidimensional degenerate parabolic equations. *J. Math. Anal. Applic.*, **210**:598–608, 1997.
[35] A.I. Vol'pert and S.I. Hudjaev. Cauchy's problem for degenerate second order quasilinear parabolic equations. *Math. USSR Sbornik*, **7**(3):365–387, 1969.
[36] M.F. Wheeler, W.A. Kinton, and C.N. Dawson. Time-splitting for advection-dominated parabolic problems in one space variable. *Comm. Appl. Numer. Methods.*, **4**:413–423, 1988.
[37] Z. Wu and J. Yin. Some properties of functions in BV_x and their applications to the uniqueness of solutions for degenerate quasilinear parabolic equations. *Northeastern Math. J.*, **5**(4):395–422, 1989.
[38] L.-A. Ying. Viscous splitting for the unbounded problem of the Navier–Stokes equations. *Math. Comp.*, **55**:89–113, 1990.

(Steinar Evje)
Department of Mathematics
University of Bergen
Johs. Brunsgt. 12
N–5008 Bergen, Norway
E-mail address: steinar.evje@mi.uib.no

(Kenneth Hvistendahl Karlsen)
Department of Mathematics
University of Bergen
Johs. Brunsgt. 12
N–5008 Bergen, Norway
E-mail address: kenneth.karlsen@mi.uib.no

(Knut–Andreas Lie)
Department of Mathematical Sciences
Norwegian University of Science and Technology
N–7034 Trondheim, Norway
E-mail address: andreas@math.ntnu.no

(Nils Henrik Risebro)
Department of Mathematics
University of Oslo
P.O. Box 1053, Blindern
N–0316 Oslo, Norway
E-mail address: nilshr@math.uio.no